ASSESSMENT OF EXTENSIONAL UNCERTAINTY MODELED BY RANDOM SETS ON SEGMENTED OBJECTS FROM REMOTE SENSING IMAGES

X. Zhao [a, b], X. Chen [a, c, *], L. Tian [a], T. Wang [b], A. Stein [b]

[a] State Key Laboratory of Information Engineering in Surveying, Mapping and Remote Sensing, Wuhan University, Luo Yu road 129, China – (cxl, tianliqiao)@lmars.whu.edu.cn

[b] International Institute for Geo-Information Science and Earth Observation, Hengelosestraat 99, Enschede, Netherlands – (xzhao, tiejun, stein)@itc.nl

c The Key Lab of Poyang Lake Ecological Environment and Resource Development, Jiangxi Normal University, Nanchang, Jiangxi, China

Commission II, WG II/4

KEY WORDS: accuracy assessment, uncertainty, random set, image segmentation, Poyang Lake

ABSTRACT:

A newly developed random set model has been applied to model the extensional uncertainty of a wetland patch. The objective of this research is to explore the corresponding variables collected on the ground for validating the uncertain image objects and to report the quality of the random set modeling. The independent samples t-test and a correlation analysis have been used to identify the main variables, whereas the overall accuracy and Kappa coefficients quantify the quality of the random set model. The results show that significant correlations exist among covering function, *Carex* coverage and NDVI. This suggests that the covering function of the random set can be quantified and interpreted adequately by NDVI derived from satellite images and *Carex* coverage measured in the field. In addition, the core set of the random set has an overall accuracy of 85 percent and a Kappa value equal 0.54, being higher than the median set and support set. We conclude that the random sets modeling of uncertainty allows us to perform an adequate accuracy analysis.

1. INTRODUCTION

Conventional pixel-based and object-based classification approaches generate maps with exclusive categories. These hard classifications are designed for mapping discrete objects and clear bounded land cover, but they are not appropriate for mapping continuous landscapes in nature such as wetlands (Woodcock and Gopal 2000). The limitation of hard classification to represent transition zones and uncertain boundaries has been a motivating factor for the development of alternative approaches based on uncertainty handling theories such as fuzzy set theory (Zadeh 1965) and random set theory (Matheron 1975; Cressie 1993). A number of soft classification and uncertainty modeling methods have been developed for classifying and representing nature landscapes such as beach (Van de Vlag and Stein 2007) and grassland (Zhao et al. 2009a), and for modeling dynamic phenomena such as fire spread (Vorob'ov 1996) and flooding (Stein et al. 2009a).

The accuracy assessment of soft classification results, however, remains a theoretical and practical difficulty. Foody (2002) gave overviews on accuracy assessment issues and current challenges. For the pixel-based soft classification, such as fuzzy classification, some research managed to perform validation by fuzzy confusion matrix which was extended from conventional assessment approach (Woodcock and Gopal 2000). Accuracy assessment of extracted image objects by object-based classification or segmentation has bigger challenge (Zhan et al. 2005), especially when objects are uncertain (Stein et al. 2009b). The main difficulty is that the information about uncertainty represented in the results does not always have corresponding objects in the field. This is because even on the ground, due to vague and unambiguous boundaries, the delineation of uncertain objects like a city may be impossible. In addition, detailed reference data which is critical for validating soft classification and uncertainty modeling results, are often unavailable, especially when the historical field data was only collected for hard classification.

Extensional uncertainty refers to the uncertainty in identifying the geometric elements that describe the spatial extent of the object (Molenaar 1998). Zhao et al. (2009b) have applied the random set model to represent extensional uncertainty of extracted image object from Landsat TM image in 2004. The accuracy of the random set model derived from a historical image is difficult to assess. Since the synchronous data with detailed information are of a significant importance for assessing model uncertainty, a clean and almost synchronous HJ-1A image with comparable spatial resolution (i.e., 30 m) two days before the survey was acquired. Moreover, the sampling plan was specially designed for investigating zonation pattern of wetland grassland and for accuracy assessment of random set model before ground survey. The objective of this research is twofold: (1) to explore the corresponding measurable variables collected on the ground for validating the uncertain image objects modeled by random sets, (2) to quantify the quality of the random set modeling results.

* Corresponding author.

2. METHODS

2.1 Study Area and Image Pre-processing

The study area PLNNR (29°05′ - 29°18′ N, 115°53′ -116°10′ E) is located to the northwest of the Poyang Lake in the JiangXi province, central China. Nine lakes in the PLNNR are connected to the Poyang Lake during the high water levels in summer and disconnected when water levels are low in spring, autumn and winter. All kinds of wetland vegetation are blooming in spring and serve as important habitats and forages for spring migrating birds. In the summer flooding time, grasses growing at high elevations (e.g., *Miscanthus*) remain stand above the water, whereas sedges (e.g., *Carex*) and submerged aquatic species (e.g., *Potamogeton*) at lower elevations are flooded beneath. When the flood is gone and winter migration birds arrive in autumn from late September, only few kinds of vegetation like *Carex* start to turn green again and thrive until winter come. Other vegetation communities become senescent in autumn and dead in winter. When sedges at the lower elevations are shooting up gradually, different kinds of birds forage on leaves and rhizomes of young sedges and rhizomes of submerged aquatic species in different elevation zones. Taller sedges also provide bird's habitat and shelter (Wu and Ji 2002). Wetland grassland has biggest width of zonation and also largest area in Banghu, therefore, our ground survey was carried out surrounding Banghu lake.

HJ-1A/B satellites were launched on Sept 6, 2008 from China. One scene of a HJ-1A image on November 24, 2009 with 30m resolution was applied and downloaded from the China Centre for Resource Satellite Data and Applications (CRESDA). As a second level product, radiometric correction and systematic geometric correction have been done before downloading and the image is under UTM WGS84 projection. A topographic map of scale 1:10,000 in PLNNR was used as the geographic reference data for more accurate geometric correction. The root mean squared error of the geometric correction was less than 10 m. The Normalized Difference Vegetation Index (NDVI) was calculated for the HJ image:

$$\mathrm{NDVI}=\frac{\rho_{nir}-\rho_{red}}{\rho_{nir}+\rho_{red}} \quad (1)$$

where ρ_{red} and ρ_{nir} stand for the spectral reflectance measurements acquired in the red and near-infrared band, respectively.

2.2 Ground Survey

From October 26th until November 6th, 2009, a ground survey was carried out around Banghu lake to investigate the zonation pattern of wetland grassland. Although it is assumed that for a random set modeling, some versions of random sampling preferably stratified unaligned random sampling be used rather than a systematic sampling. But in order to verify the gradual change of vegetation and restricted by accessibility and costs, four typical transects have been designed, starting from the river bank and perpendicularly crossing different zonations until they reach the lake bank of Banghu (Fig. 1). These four transects have 27, 24, 14, 8 sample plots respectively, so that 73 plots have been sampled in total.

Sample plots with size of 30m * 30m are distributed evenly along transects, and were fixed by measuring tape. The location of each sample plot was measured by GPS at the centre of the square, with the accuracy less than 10 m. Within the plots, the following variables were recorded: land cover types, vegetation types (communities or species), vegetation height, percent vegetation cover and bird signs such as drops and falling feather. Furthermore, five or eight subplots (1m * 1m) were also established within some 30m * 30m plots to measure the less homogeneous plots and took averaged variables. The spectral characteristics of typical vegetation types were measured within 1m * 1m subplots using SVC field-portable spectroradiometer. For each reading of the spectroradiometer, around 30 separate measurements were taken, which were then averaged for each 1m * 1m subplot.

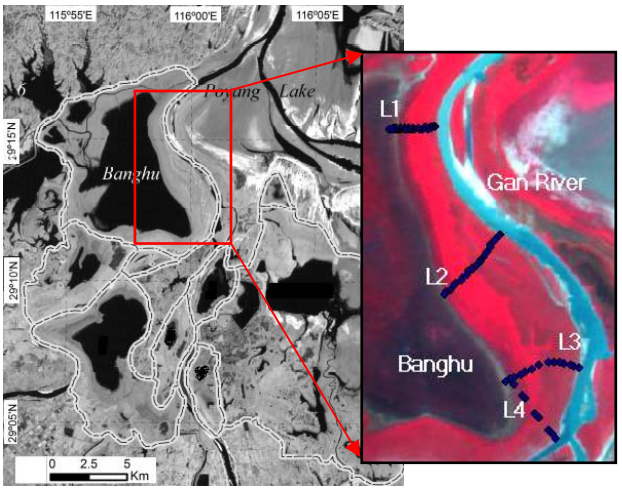

Fig. 1. Nine lakes in Poyang Lake National Nature Reserve (dish line on the left figure) and sample plots along four transects (L1-L4) on false colour HJ image (blue dots on the right figure).

2.3 Image segmentation and extensional uncertainty modelling

Random set theory has been employed as a foundation for the study of randomly varying populations and randomly varying geometrical shapes (Stoyan and Stoyan 1994) and thus applied in our previous research for modelling extensional uncertainty of image objects (Zhao et al. 2009a). In this research, our target object is the *Carex* patch which is located on the east bank of Banghu (Fig. 1). Since *Carex* is the dominant green vegetation in October, we use NDVI image as input for the region growing segmentation. Based on a threshold range (minimum and maximum pixel values), the region growing algorithm expands from a small seed combining connected pixels within pre-specified limits (Russ 2007). Vegetation patches with vague boundaries are sensitive to the setting of parameters in the region growing algorithm. Therefore, by slightly changing the parameters, e.g., under normal distribution with a small value of variance, and segmenting iteratively, a set of resulting objects established a random set (Zhao et al. 2009a; b). The image object with extensional uncertainty thus was modeled by the generated random set.

The procedure is as follows: Firstly, the growing seed was selected inside the central interior part of the target object. Then we initialized the parameters, i.e., upper and lower threshold. For each parameter, a random number was generated from a normal distribution with the initialized parameter as the mean and a preset variance. Fourthly, start the segmentation and obtain object O_i as one sample of the random set. Iterating the above steps several times and a set of resulting objects establish

a random set. Several characteristics of random set can be used to describe the extensional uncertainty of objects. For example, n polygons resulting from n times segmentation are samples of the random set, denoted as $O_1, \ldots, O_n$. The probability that pixel $x \in R^2$ occupied by the random region can be determined by $\Pr_{\bigcup_{i=1}^{n} O_i(x)}$. An estimator of the covering function of random set Γ is obtained as:

$$\Pr_{\Gamma}(x) = \frac{1}{n}\sum_{i=1}^{n} I_{O_i}(x), x \in R^2 \qquad (2)$$

Where $I_{O_i}(x)$ is the indicator function of $O_i(x)$. The covering function can be interpreted as the probability of the pixel x on space R^2 being covered by the random set. All the pixels with covering function equal to or larger than p construct a p-level set of the random set. The 0-level set, 0.5-level set and 1-level set are called support set, median set and core set respectively. In practice, we can adjust the support set to 0.05-level set and core set to 0.95-level set, in order to avoid extreme outliers. Further theoretical details about random set models and technical details about segmentation can be found in our previous work (Zhao et al. 2009a; b).

After analyzing the field data, we found that pixels with pure *Carex* have maximum NDVI values around 0.6, whereas 50 percent *Carex* coverage corresponds to NDVI values around 0.45. Since plots with NDVI larger than 0.6 are dominated by *Carex*, to simplify the random set generation procedure, we fixed 0.7 as the maximum threshold in region growing segmentation and do not apply randomization on it. On the other hand, we selected 0.45 as the initialized minimum threshold, and generated 100 random numbers from normal distribution with mean equal to 0.45 and σ^2 equal to 0.1. Finally, we placed the growing seed at the location of one sample plot where 100 percent *Carex* was recorded, and used the 100 randomized threshold intervals to obtain 100 objects and modelled them as a random set Γ.

2.4 Accuracy assessment

In order to validate the modelling result, all the 73 sample plots are used for accuracy assessment. The overall accuracy (OA), producer accuracy (PA), user accuracy (UA) and kappa coefficient are derived from error matrix. Each of these provides a different summary of the information contained in the error matrix. A widely applied kappa z-test (Congalton et al. 1983) is also used to test for statistically significant differences in accuracy of outputs. Independent samples t-tests in SPSS software were adopted to determine if the mean value of the *Carex* coverage is different for sample plots which are included and excluded by the median set. Moreover, correlation between *Carex* coverage, NDVI and covering function value were quantified by regression models.

3. RESULTS

3.1 Ground survey

From the river bank to the lake bank, transects L2-4 are approximately 2000 m long, whereas L1 is approximately 1200 m. Three different zones occur along all the four transects. The first zone is on the river bank. Flowered *Miscanthus* of 1-2 m height appears at high elevations near the river bank, often mixed with *Cynodon*, *Carex*, *Polygonum*, and human planted poplar. Some of the flowered *Miscanthus* also has green leaves of lower height, or some shorter *Miscanthus* is not flowered, we call them green *Miscanthus* in this paper. If large number of cattle graze on *Carex*, as for example in L2, the *Miscanthus* is cut to approximately 0.5 m. The second zone is *Carex* dominant zones, which across approximately 500 m horizontal distance. The height of *Carex* ranges from 0.3 to 0.6 m, and they thrive, with very high density. As forward to the lake bank, the height and density of *Carex* are decreasing and *Polygonum*, *Artemisia* and *Eleocharis* appear and mixed with it. The third zone is near the lake bank where elevation changes gradually. The indicators of low elevation are high soil moisture and plant like *Cardamine* and young *Carex*. The farthest place we reached on the lake bank in L1 is covered by 10 cm shallow water and dead *Potamogeton* and *Vallisneria* beneath. We found birds' drops and feathers frequently and the birdcall is very clear. On the bank of L2-4, we found wet soil, *Cardamine*, dead and dry *Potamogeton* and *Vallisneria* covered on soil, and shooting up *Carex* with very low density.

Figure 2 shows dominant vegetation types and their coverage at 27 sample plots along transect L1. As illustrated in the legend, the length of the bar indicates the percent coverage of vegetation which is averaged from 5 or 8 subplots. The average height of each vegetation type can be read from the centre point of the bar according to the scale on the left. For the three zonations we categorized above, samples from 1 to 5 belong to the first zone, and samples from 20 to 27 belong to the third zone. Samples from 6 to 12 are relatively homogenous and belong to the second zone, whereas samples from 13 to 17 are in transition area. From the NDVI values extracted from HJ image at corresponding sample plots, we found the NDVI achieve the peak around 0.6 at sample 8 until sample 12, where either homogenous *Carex* plots appear or *Carex* mixed with green *Miscanthus*. As the *Carex* goes shorter forward the lake, the coverage of wet soil and dead *Potamogeton* increase and NDVI values reduce to 0.2 and remain stable.

3.2 Corresponding variable in the field

In the ground survey, we measured as many variables as we can in 1m * 1m subplots, including land cover type, vegetation species, percent coverage, height and spectral curve, to detail the field information for accuracy assessment. We compares field measured NDVI values of vegetation, to which different vegetation types, coverage and heights contribute differently. First of all, plots covered by lower percent vegetation coverage will have lower NDVI. The cases of *Carex* with coverage 100, 70, 30, 5 percents show obviously decreasing NDVI. Secondly, vegetation with different heights may have the same NDVI. For example, pure *Carex* plots with height between 0.4 and 0.6 meter are have the same NDVI value 0.89. The possible reason is *Carex* extremely thrive at that heights and with very high growing density, which cause NDVI be fully saturated. Thirdly, for cases where NDVI does not achieve saturation, e.g. four *Miscanthus* plots with 100 percent coverage, the height of the plant shows its impact on NDVI. We measured both the height of flowered part and green leaves part of *Miscanthus*. The flowered parts of *Miscanthus* are dry in autumn, thus having low NDVI around

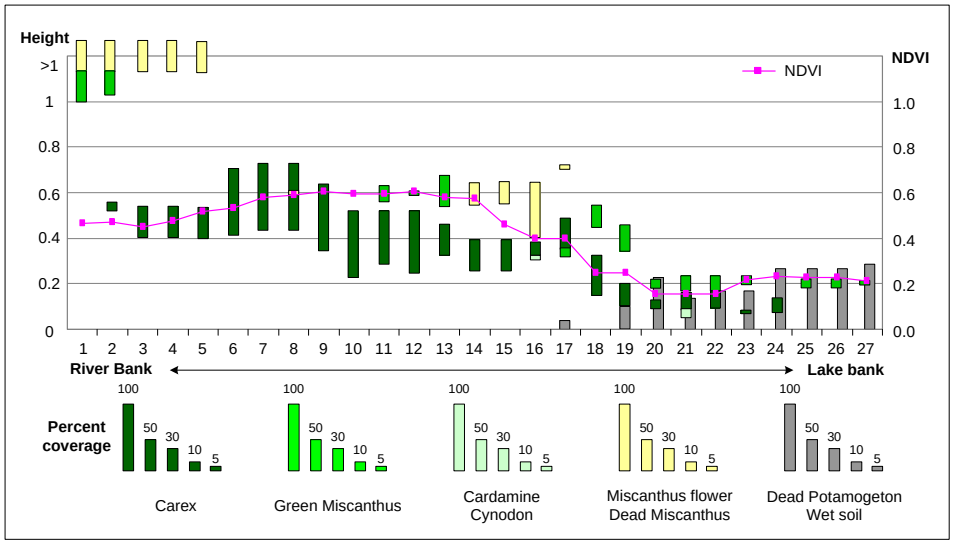

Fig. 2. Types of dominant vegetation, their percent coverage and heights along transect L1 are compared with NDVI extracted from corresponding pixels at field samples

0.25. Since the NDVI is not saturated when flowered part exist, the NDVI values reduce as heights of their green leave part decreasing. Last but not least, vegetation growing density also influences the NDVI value. For example, *Artemisia* is kind of plant which also thrive in autumn, but with very low proportion and usually mixed with *Carex*. For plots which are fully covered by *Carex* and *Artemisia* at the same height of 0.4 meter, *Artemisia* has lower NDVI of 0.79 compared with 0.89 for *Carex*. The possible reason is that coverage percent only reflects the proportion of the projected canopy of vegetation on the ground, so that *Carex* with high density has larger NDVI than *Artemisia*.

According to the results above, we found that *Carex* coverage is an outstanding variable which is closely related to NDVI, may act as the corresponding variable of covering function derived from the random set model. For the other variables, they are closely related with each other when contributing to NDVI value and can not be act as independent variable.

3.3 Extensional uncertainty modelled by random sets

Main Characteristics of random set Γ, including the covering function, the support set, the median set, the core set and the variance, were estimated. The contours of support, median illustrated in Fig. 3a indicate the possible spatial extension of this *Carex* patch with above 0.05 probabilities and above 0.5 probabilities respectively. The pixels with covering function value larger than 0.95 are enclosed by the contour of core set which almost ensure the pixel belonging to *Carex* patch. The differences between the spatial extension of support set and core set indicate the extensional uncertainty of *Carex* patch. The higher uncertainty corresponds to higher variance of random set in Fig. 3b.

3.4 Linking covering function to *Carex* coverage

By plotting the field data and estimated covering function, the values of the covering function (CF) were compared with NDVI and percent coverage of *Carex* (PCC) for all the sample plots, among which in transect L1 are shown in Fig. 4.

We found that these three curves have similar trends along the transect L1. They have peak values approximately from sample 6 to 12 and low values at the two ends. Both curves of CF and NDVI have relatively gentle slope from sample 1 to 7, compared with steep slope from sample 15 to 27. But PCC decreases rapidly from sample 6 to sample 1, making a steep slope at the left end of the curve. This mismatch can be explained by the mixture of green *Miscanthus* with *Carex* (Fig. 2), which also contribute to the NDVI. At the right end of the curves, although PCC has values around 20 percent, but due to the low height and low density of young *Carex* (Fig. 2) contributing little to NDVI value, the CF shows 0 values from sample 18 to sample 27.

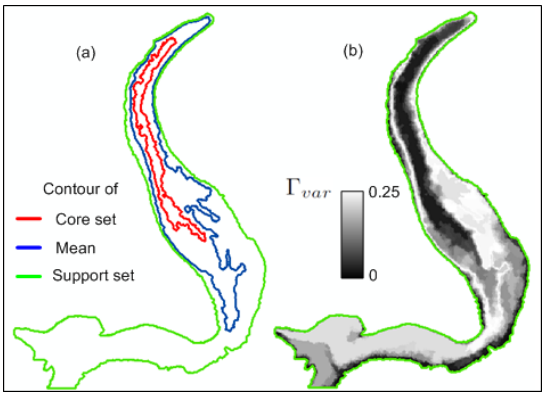

Fig. 3. Extracted object and its extensional uncertainty described by concepts from random set theory: (a) support set, median and core set (b) variance

T-test was then used to explore the relationship between median set and *Carex* coverage. The null hypothesis is that the mean value of the *Carex* coverage of samples which included by the median set is equal to the mean value of the *Carex* coverage of samples which excluded by the median set. The two-tailed p value associated with the test p = 0.000 which is smaller than 0.05, then we reject the null hypothesis. That implies that there is sufficient evidence to conclude that samples included and excluded by the median set have different *Carex* coverage.

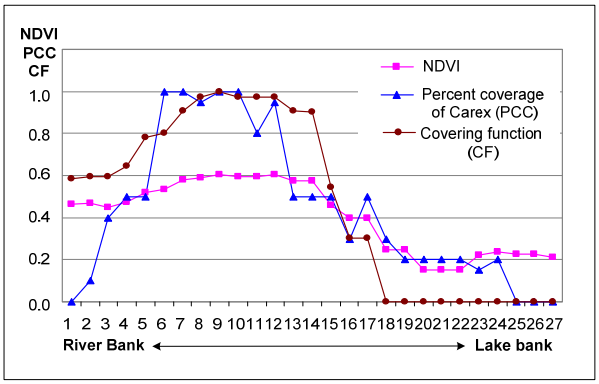

Fig. 4. Percent coverage of *Carex*, NDVI and covering function at sample plots compared along transect L1

Table 1 highlights that the correlations between covering function and *Carex* coverage were observed with the R^2-values ranging from 0.46 to 0.71, whereas correlations between covering function and NDVI have higher R^2-values ranging from 0.82 to 0.97. For the total 73 samples, although *Carex* coverage has lower R^2-value with covering function than with NDVI, but it still explains 54% of variation in covering function and the relationship is significant at 0.01 confidence level. This relationship suggests that covering function of the random set can be quantified and interpreted adequately by either NDVI from image or *Carex* coverage from the field data. The relationship between *Carex* coverage and NDVI with 0.56 R^2-value suggests that NDVI is closely related to *Carex* coverage at the time the image acquired. This result also supports our previous decision that using NDVI image as input to extract *Carex* patch.

Table 1. R^2-values of the correlation relationships between covering function (CF) and percent coverage of *Carex* (PCC) and NDVI for four transects separately and in total

Transect	L1	L2	L3	L4	L1-L4
CF-PCC	0.67	0.51	0.71	0.46	0.54
CF-NDVI	0.97	0.91	0.82	0.91	0.93
PCC-NDVI	0.63	0.62	0.63	0.48	0.56

3.5 Accuracy assessment of the extracted uncertain object

In order to validate the uncertain object, percent coverage of *Carex* recorded for each sample plot were used to group testing samples. The accuracy assessment was applied to the support set by comparing with all the samples where *Carex* appears, to the median set by samples where above 50 percent of area is dominated by *Carex*, and to the core set by samples which are 95 percent covered by *Carex*. In each error matrix, number of samples belongs to tow classes: presence of *Carex* and absence of *Carex* are indentified. Table 2 details the mapping accuracy of the support set, the median set and the core set by OA, PA, UA and kappa coefficient derived from error matrix. The highest overall accuracy was achieved by the core set with OA of 85 percent and kappa 0.54. According to (Mather 1999), the core set and the median set have moderate kappa value, whereas the support set has poor kappa value. By further looking at each class, we find that presence and absence of *Carex* has high PA and UA for support set and core set respectively, which indicate that these two classes are reliable in support set and core set respectively. Presence of *Carex* has high UA and low PA in core set, showing that there is more area of *Carex* in the field than is indicated by the core set. Absence of *Carex* has both low PA and UA in support set, because 12 out of 16 samples which are classified as absence correspond to presence in the field data. The possible explanation for the unsatisfied accuracy is that the grouping criteria of making testing samples for the support set is not appropriate. We get supporting evidences from sample 18 to sample 24 in Fig. 4. These samples have 0 covering function, and not belong to the support set, but they still have 20 percent *Carex* at low height and with low density. This result suggests that the support set is not sensitive to the *Carex* coverage lower than 20 percent.

A kappa z-test for pair-wise comparison in accuracy shows that there was significant difference between the support set and other sets, but no significant difference between the core set and the median set. The results suggest the quality of the core set and the median set is significantly higher than that of the support set.

Table 2. Comparison of OA, UA, PA and kappa coefficients for the core set, the median and the support set. C1 indicates class presence of *Carex* and C2 for class absence of *Carex*.

Core set	PA (%)	UA (%)	OA (%)	Kappa
C1	47	90	85	0.54
C2	98	84		
Median set				
C1	76	85	77	0.52
C2	78	66		
Support set				
C1	82	93	78	0.22
C2	50	25		

4. CONCLUSION AND DISCUSSION

In this research, we applied the random set model for representing uncertain boundary of a *Carex* patch, and perform accuracy assessment on the modelling results. We found that *Carex* coverage can be the corresponding variable collected on the ground, by which the covering function of random sets can be quantified and interpreted adequately. The core set of the random set has higher accuracy than the median set and the support set.

Significant correlations were found among covering function, *Carex* coverage and NDVI, which suggests that covering function of the random set can be quantified and interpreted adequately by NDVI derived from image and *Carex* coverage measured in the field. For the other variables, such as vegetation types, height and density and coverage, they also influence the modelling result, and should be considered together. These variables, however, may belong to different scales, such as nominal (e.g. vegetation type), ordinal (e.g. big or small density) and ratio scale (e.g. height and coverage). So they are difficult to integrate into one general variable which might be better match with the covering function of random set.

The quality of the random set models was assessed quantitatively by OA, UA, PA and the kappa coefficients.

The accuracy of core set is better than that of the median set and much better than that of the support set. Since the support set is not sensitive to the young *Carex* with coverage less than 20 percent, inappropriate criteria for grouping test samples might be the reason for its poor accuracy. This result suggests that the random set model has a better performance on the high coverage area and criteria for validating the support set should be determined not only based on the coverage. Moreover, it supports that *Carex* coverage cannot be the only variable fully explaining the covering function and other variables such as height should be considered especially when the coverage is low.

The accuracy of random set model applied in this study is just moderate according to the assessment report. Several reasons could contribute: on one hand, the parameters in the region growing segmentation algorithm need further adjustments. On the other hand, the field data which are often referred as the ground truth may not perfectly match with modeling results. In this study, more factors such as heights and density of vegetation should be integrated with vegetation coverage as united reference data for accuracy assessment.

ACKNOWLEDGEMENTS

This Research is funded by the 973 Program (Grant No. 2009CB723905), Sino-Germany Joint Project (Grant No. 2006DFB91920), National Key Project of Scientific and Technical Supporting Programs (2007BAC23B05) and NSFC project (Grant No. 40721001). The authors would like to express their many thanks to CRESDA for providing HJ image and Mr. Lian Feng, Mr. Xiaobing, Cai and Mr. Shoujing, Yi for their assistants in the ground survey.

REFERENCES

Congalton, R. G., R. G. Oderwald and R. A. Mead, 1983. Assessing Landsat classification accuracy using discrete multivariate analysis statistical techniques. *Photogrammetric Engineering & Remote Sensing*, 49, pp. 1661-1668.

Cressie, N. A. C., 1993. Statistics for spatial data(eds.). Wiley-Interscience, pp. 725-803.

Foody, G. M., 2002. Status of land cover classification accuracy assessment. *Remote Sensing of Environment*, 80, pp. 185-201.

Mather, P. M., 1999. Land cover classification revisited. *Adances in remote sensing and GIS analysis*. P. M. Tate and N. J. Tate (eds.). Wiley, Chichester, pp. 7-16.

Matheron, G., 1975. *Random sets and integral geometry*. New York: Wiley.

Molenaar, M., 1998. *An Introduction to the Theory of Spatial Object Modeling for GIS*. Taylor & Francis.

Nguyen, H. T., 2006. *An Introduction to Random Sets*. Chapman Hall.

Pal, N. R. and S. K. Pal, 1993. A review on image segementation techniques. *Pattern Recognition*, 26, pp. 1277-1294.

Russ, J. C., 2007. *The Image Processing Handbook*. Taylor & Francis.

Stein, A., P. Budde and M. Z. Yifru, 2009a. Stereology for Multitemporal Images with an Application to Flooding. *Research Trends in Geographic Information Science*. G. Navratil (eds.). Springer-Verlag, pp. 135-150.

Stein, A., N. A. S. Hamm and Y. Qinghua, 2009b. Handling uncertainties in image mining for remote sensing studies. *International Journal of Remote Sensing*, 30, pp. 5365-5382.

Stoyan, D. and H. Stoyan, 1994. *Fractals, Random Shapes and Point Fields*. John Wiley&Sons.

Van de Vlag, D. E. and A. Stein, 2007. Incorporating uncertainty via hierarchical classification using fuzzy decision trees. *IEEE Transactions on geoscience and remote sensing*, 45(1), pp. 237-245.

Vorob'ov, 1996. Random set models of fire spread. *Fire technology*, 32(2), pp. 137-173.

Woodcock, C. and S. Gopal, 2000. Fuzzy set theory and thematic maps: accuracy assessment and area estimation. *International Journal of Geographical Information Science*, 14(2), pp. 153-172.

Wu, Y. and W. Ji, 2002. *Study on Jiangxi Poyang Lake National Nature Reserve*. China Forestry Publishing House Beijing.

Zadeh, L. A., 1965. Fuzzy sets. *Information and Control*, 8, pp. 338-353.

Zhan, Q., M. Molenaar, K. Tempfli and W. Shi, 2005. Quality assessment for geo-spatial objects derived from remotely sensed data. *International Journal of Remote Sensing*, 26(14), pp. 2953-2974.

Zhao, X., A. Stein and X. Chen, 2009a. Application of random sets to model uncertainties of natural entities extracted from remote sensing images. *Stochastic Environmental Research and Risk Assessment*. 10.1007/s00477-009-0358-3

Zhao, X., A. Stein and X. Chen, 2009b. Quantification of Extensional Uncertainty of Segmented Image Objects by Random Sets. *IEEE Transactions on geoscience and remote sensing*. (under review)